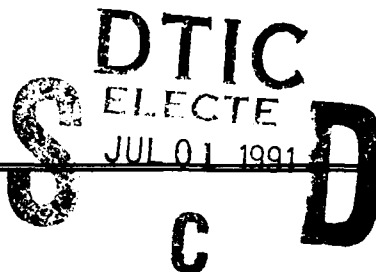


AD-A237 463



2

## Quarterly Letter Report

### Growth, Characterization and Device Development in Monocrystalline Diamond Films

Supported by the Innovative Science and Technology Office  
Strategic Defense Initiative Organization  
Office of Naval Research  
under Contract #N00014-90-J-1604  
for the period April 1, 1991-June 30, 1991

Robert F. Davis, Jeffrey T. Glass, Klaus J. Bachmann, and R. J. Trew\*  
North Carolina State University  
c/o Materials Science and Engineering Department and  
\*Electrical and Computer Engineering  
Raleigh, NC 27695-7907

June 30, 1991

91-03780



91 03780

# REPORT DOCUMENTATION PAGE

Form Approved  
OMB No 0704-0188

Public reporting burden for this collection of information is estimated to average 1 hour per response, including the time for reviewing instructions, searching existing data sources, gathering and maintaining the data needed, and completing and reviewing the collection of information. Send comments regarding this burden estimate or any other aspect of this collection of information, including suggestions for reducing this burden, to Washington Headquarters Services, Directorate for Information Operations and Reports, 1215 Jefferson Davis Highway, Suite 1204 Arlington, VA 22202-4302 and to the Office of Management and Budget, Paperwork Reduction Project (0704-0188) Washington, DC 20503

1. AGENCY USE ONLY (Leave blank)		2. REPORT DATE June, 1991		3. REPORT TYPE AND DATES COVERED Quarterly Letter 4/1/91-6/30/91	
4. TITLE AND SUBTITLE Growth, Characterization and Device Development in Monocrystalline Diamond Films				5. FUNDING NUMBERS s400003srr08 1114SS N00179 N66005 4B855	
6. AUTHOR(S) Robert F. Davis					
7. PERFORMING ORGANIZATION NAME(S) AND ADDRESS(ES) North Carolina State University Hillsborough Street Raleigh, NC 27695				8. PERFORMING ORGANIZATION REPORT NUMBER  N00014-90-J-1604	
9. SPONSORING / MONITORING AGENCY NAME(S) AND ADDRESS(ES) Department of the Navy Office of the Chief of Naval Research 800 North Quincy Street, Code 1513:CMB Arlington, VA 22217-5000				10. SPONSORING / MONITORING AGENCY REPORT NUMBER	
11. SUPPLEMENTARY NOTES					
12a. DISTRIBUTION / AVAILABILITY STATEMENT  Approved for Public Release; Distribution Unlimited				12b. DISTRIBUTION CODE	
13. ABSTRACT (Maximum 200 words)  Carbon has been implanted into monocrystalline (100) Cu substrates. Owing to the low solubility of C in Cu, it was easily diffused to a clean Cu surface at 550° C in the form of graphite rather than the desired diamond, as shown by Auger electron spectroscopy measurements. Laser reflection interferometry has proven to be a useful technique in the study of diamond growth processes. Nucleation and growth rates were monitored in real time. The problem of surface roughness of the polycrystalline films was surmounted by growing diamond on a thin amorphous C or diamond-like film. The microwave performance of p-type diamond MESFETs operating at 10 GHz has been investigated. The moderate activation energy of the p-type dopant of B may force operation at elevated temperature. However this may result in a significantly degraded RF performance, since holes in diamond demonstrate a T <sup>-2.8</sup> temperature dependence.					
14. SUBJECT TERMS diamond thin films, chemical vapor deposition, Raman spectroscopy, electronic devices, MESFETs, ion implantation high pressure studies, epitaxial regrowth, amorphous C films				15. NUMBER OF PAGES 25	
				16. PRICE CODE	
17. SECURITY CLASSIFICATION OF REPORT UNCLAS	18. SECURITY CLASSIFICATION OF THIS PAGE UNCLAS	19. SECURITY CLASSIFICATION OF ABSTRACT UNCLAS	20. LIMITATION OF ABSTRACT SAR		

## Table of Contents

<b>I. Growth of Carbon Films on Monocrystalline Copper</b>	<b>1</b>
A. Background	1
B. Experimental	1
C. Results and Discussion	2
D. Conclusions	5
<b>II. <i>In-Situ</i> Growth Rate Measurement and Nucleation Enhancement for Microwave Plasma CVD of Diamond</b>	<b>8</b>
<b>III. Modeling and Characterization of Electronic Devices Fabricated from Semiconducting Diamond Thin Films</b>	<b>16</b>
A. Introduction	16
B. Investigation Procedure	16
C. P-Type Semiconducting Diamond	17
D. Results	18
E. Conclusions	25
F. Future Research Plans and Goals	25
G. References	25

Accession For	
NTIS	DTIC Tab
DTIC Tab	DTIC Tab
DTIC Tab	DTIC Tab
DTIC Tab	DTIC Tab
By	
Distribution	
Availability Codes	
Dist	Avail and/or Special
A-1	

## **I. Growth of Carbon Films on Monocrystalline Copper**

### **A. Background**

Prins et. al. (presentation at the Diamond Conference in Washington D.C., Sept. 1990) reported that epitaxial diamond layers can be grown on single crystal (111) copper by means of high dose carbon ion implantation at elevated temperatures. However, Lee et. al. (presented at the Electrochemical Society Conference in Washington D.C., May 1991) recently reported that this method invariably results in a highly oriented crystalline graphite film. Narayan et. al. (Science, April 18, 1991, pp. 416-418) recently reported to have achieved a diamond film by implanting carbon ions into copper at room temperature followed by a laser-annealing method. Although Prins' method did not result in diamond, the implantation-out-diffusion method may be important in the attainment of diamond films via other process routes and merits closer study.

Copper has a lattice constant close to diamond and a very low solubility of carbon. At elevated temperatures, the implanted carbon atoms diffuse to the surface due to thermal activation and the lack of solubility in copper. As such, they may arrange themselves, under the influence of the surface crystallographic template of the host copper material, into the diamond lattice. In the approach used in this study, carbon ions were implanted into single crystal copper (100) substrates at room temperature and were subsequently out-diffused at an elevated temperature in the presence of a hydrogen plasma. The C out-diffusion was conducted in a controlled manner, which should facilitate a better understanding of the operative kinetics. X-ray Photoelectron Spectroscopy (XPS), Auger Electron Spectroscopy (AES), and Low Energy Electron Diffraction (LEED) contained in a UHV analytical system were used to study the bonding and crystalline nature of the growing carbon film.

### **B. Experimental**

A 99.999% pure, (100) oriented copper substrate, having a diameter of 0.5 inches and a thickness of 1.5mm, was electropolished and cleaned. The cleaning procedure included a thirty minute exposure to ultraviolet light to remove the hydrocarbons from the surface and a hydrofluoric acid etch to remove the oxide.  $^{12}\text{C}$  species, obtained from a  $\text{CO}_2$  source, were implanted at room temperature with a beam energy of 120keV, a beam dose of  $5 \times 10^{17}$  ions/cm<sup>2</sup>, and a beam angle of 10°. The experiments were performed in a system that couples the UHV analytical chamber noted above to a diamond growth microwave plasma chamber. The samples were characterized using the above mentioned techniques.

### C. Results & Discussion

Although the as-received copper substrate had a mirror-like appearance (prior to the implantation procedure) the crystal perfection at the surface was still unknown. Damage caused by the sawing and polishing operations introduce surface defects such as polishing streaks that can sometimes penetrate up to 10-50 $\mu$ m beneath the surface. It was deemed necessary to check the surface damage on the Cu substrates, since this could be an important barrier to achieving the heteroepitaxial growth of diamond on Cu. The method used to observe this surface damage was x-ray topography. Dr. David Black at The National Institute of Standards and Technology produced the x-ray topograph, shown in Figure 1, of one of our (100) oriented and representative copper single crystal samples. The x-ray topograph shows the large amount of surface damage produced by the cutting and polishing procedures. The damage is as deep as 50 $\mu$ m in some areas. This was probably caused by the early polishing steps. The widespread damage also indicates that the sample is not too badly strained. A method to rid the substrate of this damage (or not to produce it) must be determined.

The XPS survey scan obtained on the implanted Cu (100) substrate following the UV and HF cleaning procedures is shown in Figure 2a. All of the major Cu peaks are visible along with the C<sub>1s</sub> peak indicating the presence of C on the copper surface. This impurity C had to be removed before the out-diffusion occurred, since an absolutely clean (C-free) surface is required to reduce the probability for graphite nucleation. It should be noted that both O and F are absent in the survey scan. The hydrofluoric acid effectively removed all of the surface oxide and apparently left the surface hydrogen-terminated. All of the characterization was conducted *in-situ*, since the sample was never removed from the UHV chamber.

The next step was to remove the impurity C on the surface without thermally exciting the implanted C atoms in the bulk to diffuse to the surface. This was accomplished by heating the substrate with the help of a hydrogen plasma at 300°C for fifteen minutes. An optical pyrometer was used to measure the substrate temperature, and the sample was in a remote plasma location. Figure 2b illustrates the survey scan following this treatment. The only features present are those associated with copper - the C was effectively removed from the surface. Apparently at 300°C the C etch rate is faster than its exsolution rate and thus the surface is left free of any C. A LEED pattern was obtained at this time. It showed a p(1X1) structure which is characteristic of a clean (100) oriented face of Cu.



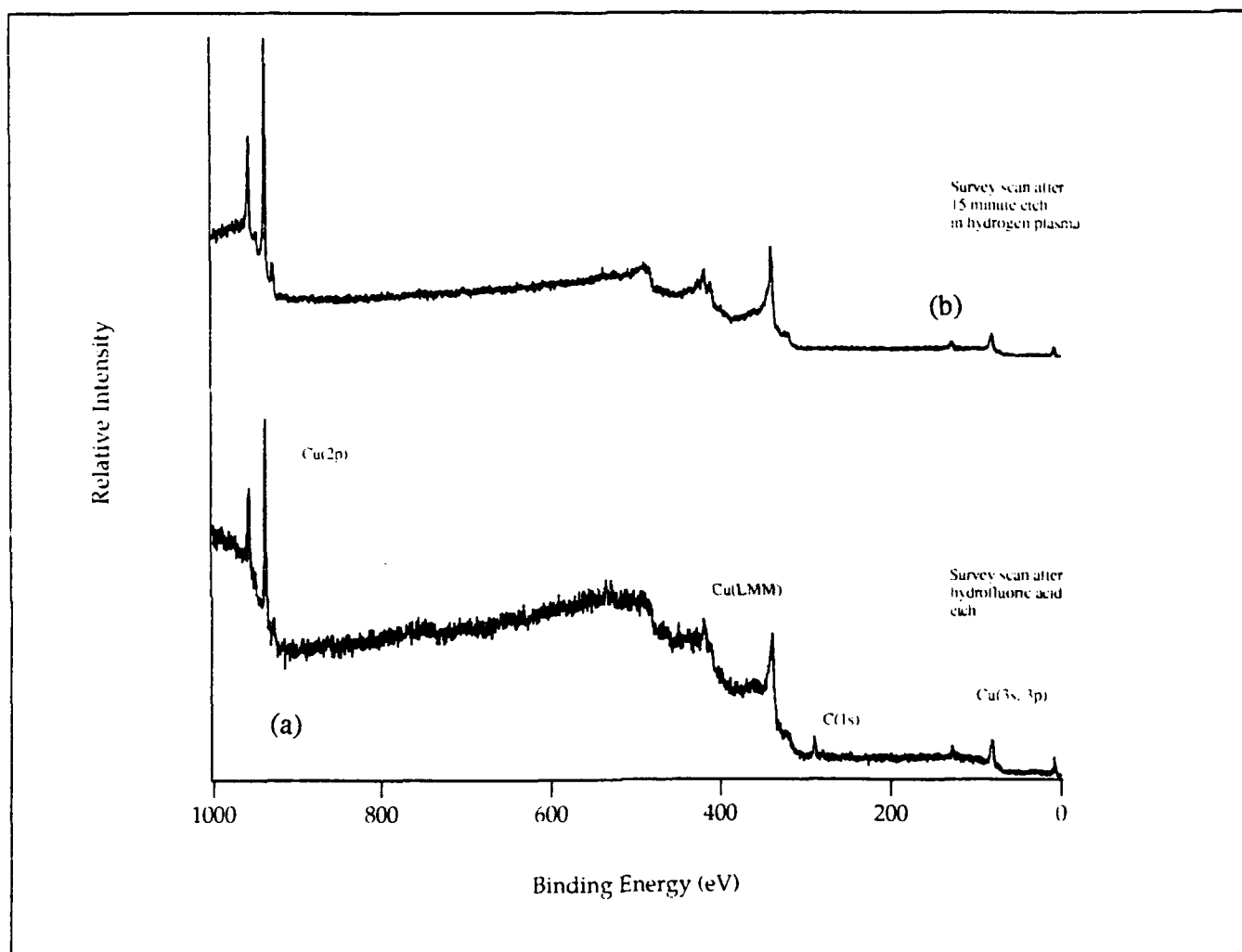


Figure 2. A comparison between the XPS scans for a (a) HF acid etched surface and (b) a clean copper surface following a 15 minute exposure to a  $H_2$  plasma.

The temperature of 550°C was chosen to exsolve the implanted C atoms from the bulk Cu. At this temperature the exsolution rate of C appears to be greater than the etch rate, therefore, yielding an over-growth. Ideally, it would be desirable to operate at a temperature where the etch rate of graphite and exsolution rate of C in the H<sub>2</sub> plasma are identical. The H<sub>2</sub> should preferentially etch away any sp<sup>2</sup> bonded graphite nuclei that form on the surface leaving behind any sp<sup>3</sup> bonded diamond nuclei, since the sp<sup>2</sup>/sp<sup>3</sup> etch rate ratio is ≈100/1. A series of growth and analysis steps followed at: 15, 30, and 300 minutes. After 15 minutes XPS spectra showed the presence of C on the surface, perhaps a fraction of a monolayer, and the LEED pattern remained p(1X1) but also included streaks which were probably due to graphite island formation on the surface. The carbon peak intensity increased with growth time, but no shifts in binding energy were observed. Figure 3 illustrates this point. The C<sub>1s</sub> peak intensity, relative to the Cu<sub>LMM</sub> absorption peak intensity, has increased following 5 hours of annealing in the H<sub>2</sub> plasma at 550°C.

Auger electron spectroscopy was used to identify the carbon polymorph present on the surface. Even at moderate resolution, this technique can be utilized to distinguish between diamond, graphite, and amorphous carbon by studying the shape of the low energy side of the carbon KLL peak (Lurie & Wilson, Surf. Sci. 65, 476, (1977)). In this case, the C present was identified as pyrolytic graphite (sp<sup>2</sup> bonding), since the C(KLL) fine structure, shown in Figure 4, has the highest intensity peak at a lower binding energy. For diamond, on the other hand, the highest intensity peak should be at a higher binding energy due to the sp<sup>3</sup> bonding. Also, the AES graphitic fine structure did not change much with time. The final LEED pattern contained a c(2X2) structure accompanied by a lobed ring structure, which is due to the presence of graphite islands.

#### D. Conclusions

Preliminary results for this approach have resulted in a graphitic surface phase. An effective cleaning method has been established for removing impurity C and O which was verified using XPS. It has been determined that at 550°C the exsolution of C occurs. In future experiments, a lower annealing temperature will be attempted in order to reach a condition where the etch rate of sp<sup>2</sup>-bonded species is at least equivalent to the C exsolution rate. Also, SIMS and SEM will be used to further characterize the implanted and annealed Cu substrates.



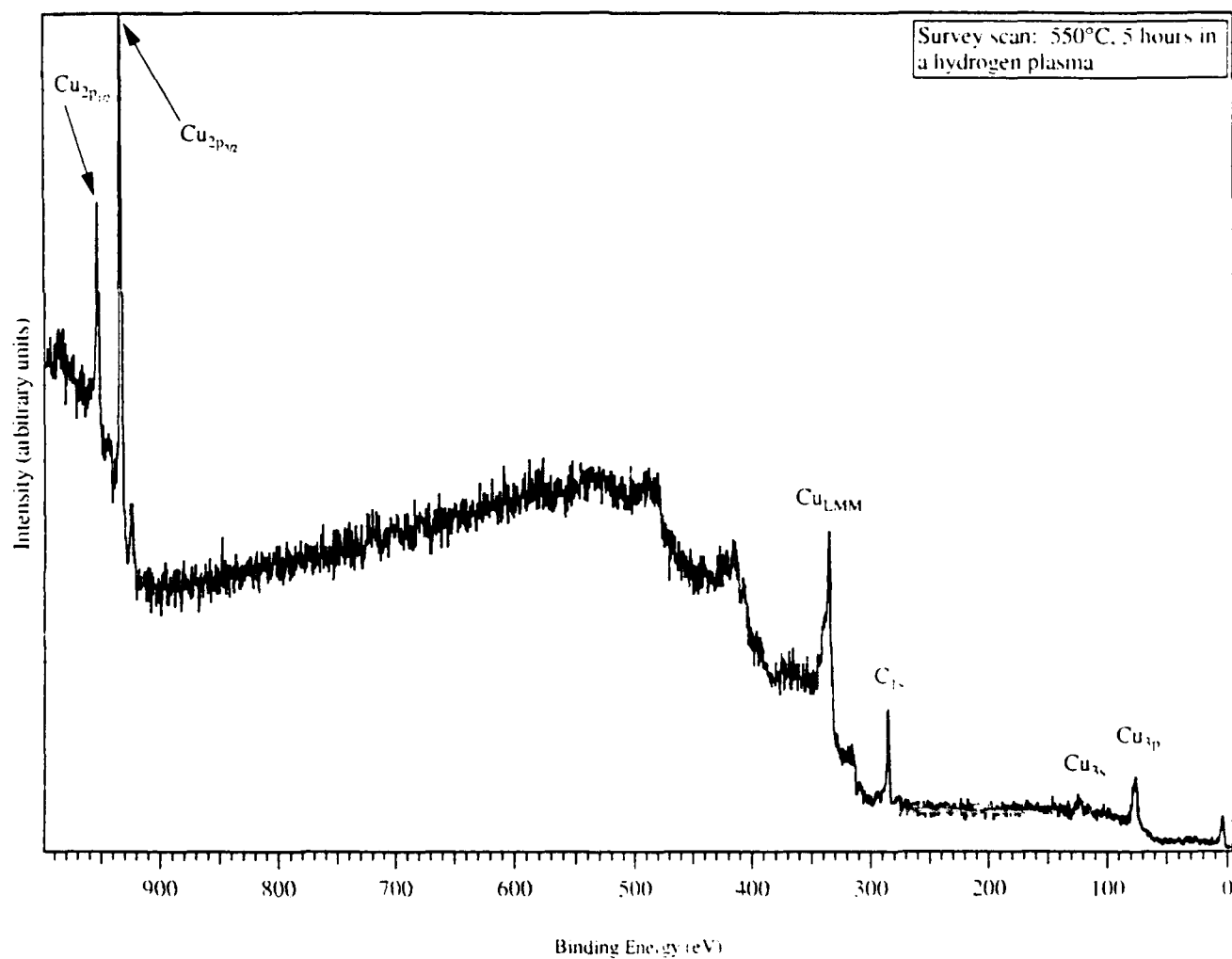


Figure 3. An XPS survey scan following 5 hours of exposure to the  $\text{H}_2$  plasma @ 550°C. Note the large  $\text{C}_{1s}$  peak relative to the  $\text{Cu}_{\text{LMM}}$  peak indicating the presence of a large amount of carbon on the surface.

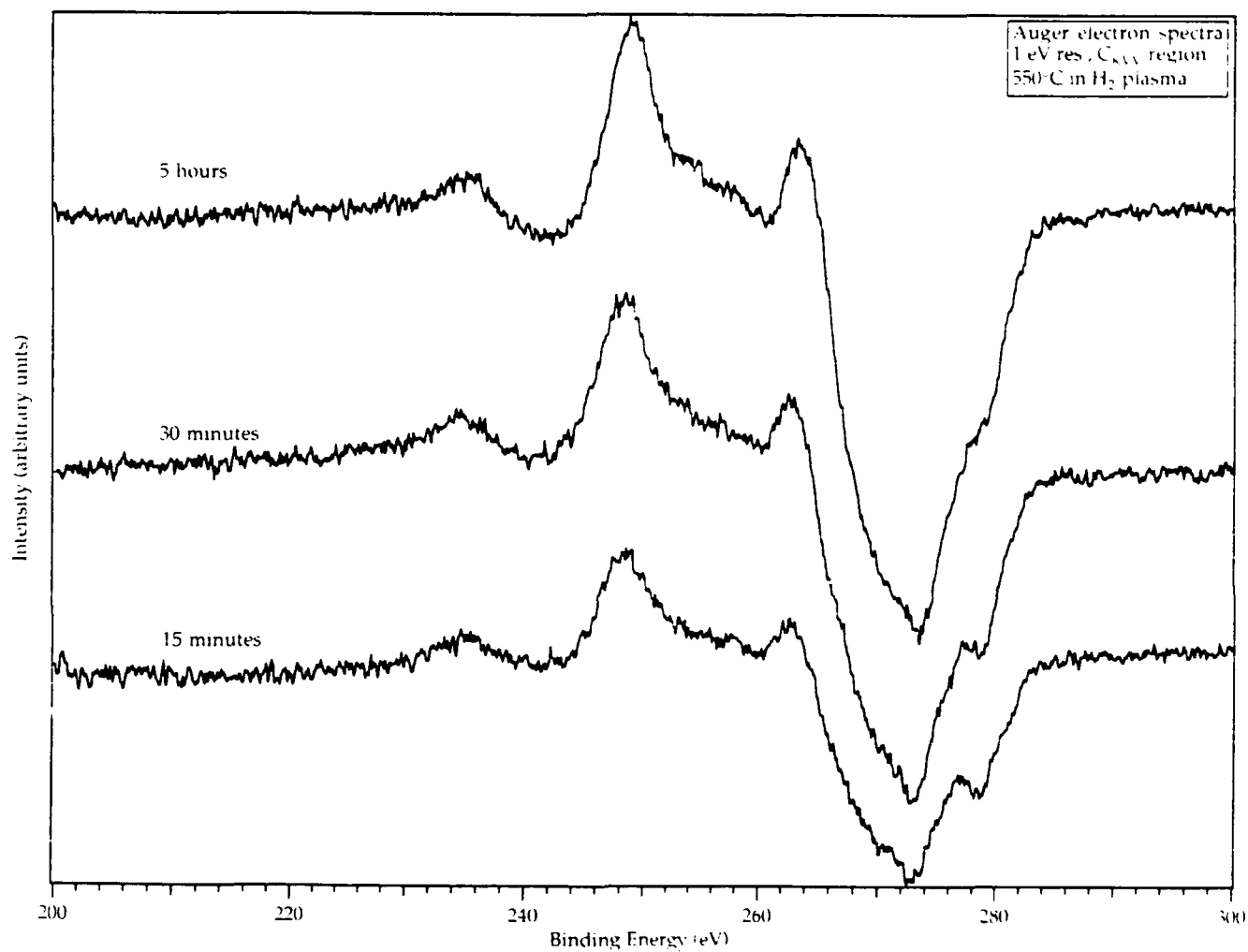


Figure 4. Auger electron spectra of the out-diffused carbon on the copper surface at 550°C and various growth times. The fine structure is characteristic of graphite.

## II. *In-Situ* Growth Rate Measurement and Nucleation Enhancement for Microwave Plasma CVD of Diamond

Laser reflection interferometry (LRI) has been shown to be a useful *in-situ* technique for measuring growth rate of diamond during microwave plasma chemical vapor deposition (MPCVD). Current alternatives to LRI usually involve *ex-situ* analysis such as cross-sectional SEM or profilometry. The ability to measure the growth rate in 'real-time' has allowed the variation of processing parameters during a single deposition and thus the extraction of much more information in a fraction of the time. In-situ monitoring of growth processes also makes it possible to perform closed loop process control with better reproducibility and quality control. Unfortunately LRI requires a relatively smooth surface to avoid surface scattering and the commensurate drop in reflected intensity. This problem was remedied by greatly enhancing the diamond particle nucleation via the deposition of an intermediate carbon layer using substrate biasing. When an unscratched silicon wafer is pretreated by biasing negatively relative to ground while in a methane-hydrogen plasma nucleation densities much higher than those achieved on scratched silicon wafers are obtained. The enhanced nucleation allows a complete film composed of small grains to form in a relatively short time, resulting in a much smoother surface than is obtained from a film grown at lower nucleation densities.

It is commonly agreed upon that the unique combination of properties which diamond films possess will lead to both the improvement of existing technologies as well as the establishment of new technologies which can not yet be envisioned.<sup>1-4</sup> In this sense, diamond is an "enabling" technology. Thus, any improvements in the current status of film processing are potentially quite valuable. In the present research such progress has been achieved by employing Laser Reflection Interferometry (LRI), which has been used previously to monitor the processing of thin films other than diamond.<sup>5-7</sup> The purpose of this letter is to show how this technique may aid the study of diamond growth, making it simpler and more efficient to perform parametric studies of growth rate responses, and eventually be used as an *in-situ* process control tool. The primary advantage of LRI, is that it makes possible the continuous monitoring of growth rates while a deposition is in progress. Thus changes in these rates during a single deposition (either due to purposeful changes in growth parameters or accidental changes due to unforeseen problems) can be determined. It also allows one to account

---

Submitted to Applied Physics Letters on April 20, 1991: B. R. Stoner, B. E. Williams, S. D. Wolter, J. T. Glass, Department of Materials Science and Engineering, North Carolina State University, Raleigh, NC 27695-7919 and K. Nishimura, Visiting from the Electronics Research Laboratory, Kobe Steel, Ltd., Kobe, Japan

for the initial "incubation" period during diamond deposition prior to the actual onset of growth.

Laser interferometry works by the simple superposition of two light waves. There is a reflection of the waves from both the top surface of the growing diamond film as well as the interface between the film and the substrate. The light waves add, and as the film continues to grow there is a cycling of the intensity due to periods of both constructive and destructive interference. Typical data of the reflected intensity as a function of time are shown in Figure 5. For monochromatic light the growth rate (GR) may be calculated as;

$$GR = (\lambda/2\eta)/T,$$

where  $\lambda$  = wavelength of the laser light

$\eta$  = index of refraction of the film

and  $T$  = period between interference cycles.

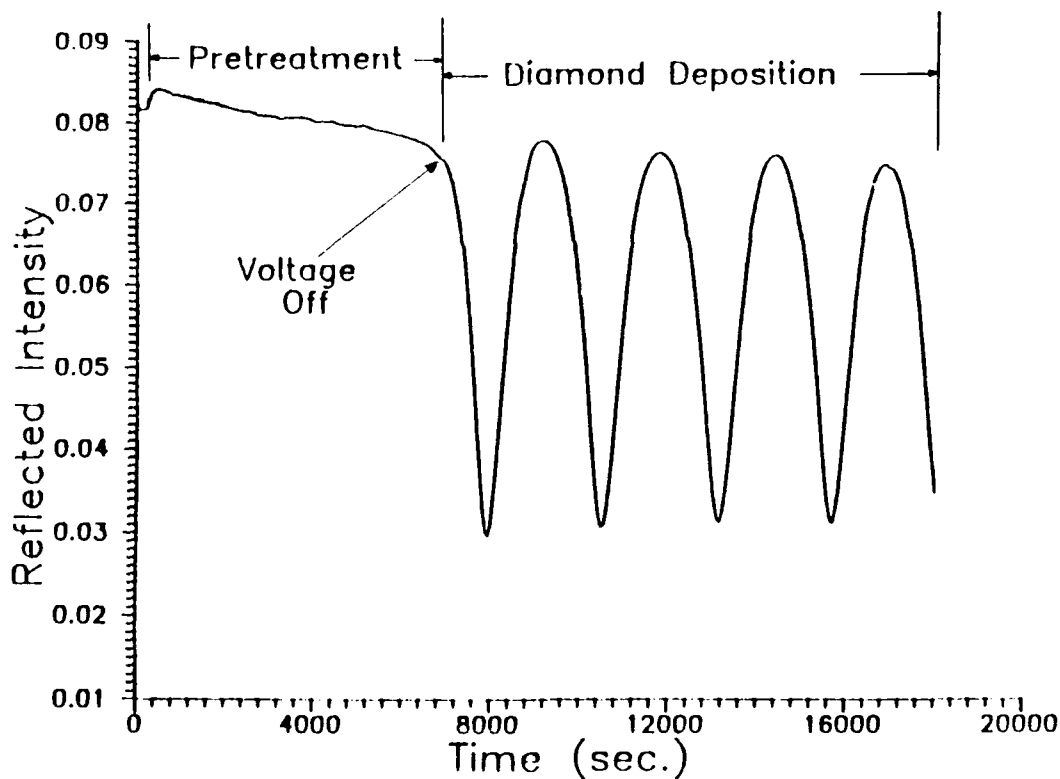


Figure 5. Typical data showing the interference cycles in the reflected intensity during diamond film growth, and the incubation period at the beginning of the deposition run.

Since the index of refraction may vary with the quality of diamond<sup>8</sup>, it is necessary to adjust the value of  $\eta$  utilizing a series of calibration experiments. This may be done by performing depositions to cover the desired extremes in relative quality (as

determined by some independent technique such as Raman Spectroscopy). Next the thicknesses of the films are independently measured and compared to those calculated from LRI. One then solves for  $\eta$  in the above equation to determine the index of refraction at those extremes.

The diamond films for this study were grown in an ASTeX, cylindrically coupled, stainless steel microwave chamber. Figure 6 shows how LRI was used to monitor the

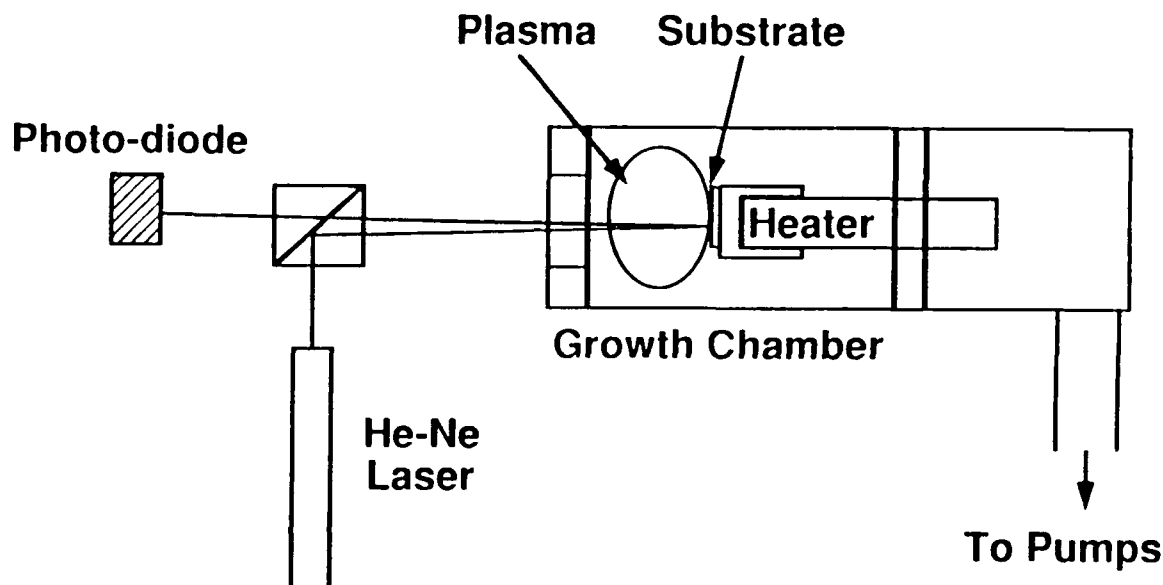


Figure 6. Diagram of the microwave plasma CVD system and the LRI apparatus.

growth rate in this system. The laser was reflected nearly perpendicular to the substrate and the reflected intensity, monitored via a silicon photo-diode, was recorded by a computer. A helium-neon laser was used ( $\lambda = 630 \text{ nm}$ ) in this study, which corresponds to  $0.13 \text{ }\mu\text{m}$  of film growth per intensity cycle (see Figure 5) in the case of a high quality diamond film with  $\eta = 2.4$ . Several initial calibration runs were performed with methane concentrations ranging from 0.5% to 5%. Even in the case of the poorest quality film, the actual thicknesses varied less than 10% for films  $1\text{--}4 \text{ }\mu\text{m}$  thick, from that measured by LRI assuming this index of refraction.

It was mentioned earlier that LRI has been previously used to measure the growth rate during thin-film epitaxial growth. The strict theory for this technique is based on a layer-by-layer increase in film thickness, and is understandably not ideally suited for measuring discrete island or polycrystalline film growth due to scattering of the laser light. This is the reason that initial attempts by the authors to measure the MPCVD growth rate of diamond on silicon using LRI had failed. Due to the relatively low nucleation density the surface was simply not smooth enough, even when optimum

diamond "scratching" was employed as a pretreatment. This lead to the biasing enhancement of nucleation density discussed below. This biasing increases the initial density of nuclei allowing a complete film to be formed more quickly, resulting in more uniform thickness than in the case where there are few initial nucleation sites. In the limiting case, where there is nucleation at every surface lattice site, the result would be the ideal layer-by-layer film growth mentioned above. This biasing allows LRI to be utilized for depositions lasting as long as 70 hours and film thicknesses greater than 7 $\mu$ m.

Previous techniques for increasing the nucleation density of diamond have been reported.<sup>9-13</sup> These techniques range from the pre-deposition of an amorphous or 'diamond-like' carbon film<sup>9-11</sup> to more efficient methods of surface abrasion.<sup>12,13</sup> Although each of these techniques was successful in enhancing nucleation density, there are several advantages to the biasing pretreatment described herein. It may be performed '*in-situ*' and thus is very convenient due to the elimination of any abrasion step. Furthermore, it is very reproducible, easy to control and the instrumentation is minimal.

The nucleation density of diamond on unscratched silicon was enhanced by biasing the substrate negatively prior to deposition, while it was immersed in the plasma. In so doing, the nucleation densities were several orders of magnitude higher than on unscratched silicon, and approximately an order of magnitude higher than on conventionally scratched silicon wafers. In the present study, bias voltage and current were approximately -250 volts and 100 mA respectively (for a 1% methane in hydrogen mixture at 15 torr), and the optimum biasing period appears to be 1 to 2 hours. The nucleation density may be controlled by either changing the time of pretreatment or varying the bias voltage.

Aside from utilizing LRI as an *in-situ* probe, this technique had several other benefits. First, it became no longer necessary to damage the as-received polished surface of the silicon wafer by abrading it with diamond paste. If heteroepitaxial growth is ever expected to be obtained, this is essential. Second, all the pretreatment may be preformed in a much more controlled, cleaner environment, where it may be directly followed by the the diamond deposition. Thus, it is possible to create a smooth transition from the pretreatment layer to the diamond film by slowly decreasing the bias voltage. A clean and graded interface of this type may help improve the adhesion of diamond films to substrates where there is a significant mismatch in the coefficient of thermal expansion. Finally, under optimum conditions the nucleation density is much higher than any other technique examined by the authors, yielding the smoothest, most uniform as-grown surface.

Almost always during low pressure CVD of diamond there is period of time in the beginning of a deposition where no film growth is observed, as discussed in Figure 5. LRI allows one to directly observe and account for this "incubation" or "nucleation" period. During the incubation period, the reflected intensity is relatively constant, but as soon as a film begins to grow, there is a noticeable decrease in the reflected intensity. This initial drop in intensity is thought to be due to the absorption of light by the surface layer of carbon which is deposited during the bias pretreatment. When this drop in intensity is observed, the pretreatment (or voltage) may be turned off, and standard diamond growth allowed to begin. If the voltage is maintained the carbon layer will continue to grow, followed by a poorer quality diamond than in the case where the bias is removed. This result is similar to that observed by Yugo et al.<sup>14</sup>, where poorer quality diamond growth was observed under negative substrate bias than under positive or no bias. It should be noted that most current methods for measuring growth rate involve dividing the resulting film thickness by the total growth time. If the nucleation period is not accounted for, then considerable error may be introduced in this growth rate determination. LRI makes it possible to measure this nucleation period as well as growth rate, either of which may vary with changes in processing parameters.

The chemical and physical nature of the pretreatment layer created by biasing is not yet fully understood; however initial in-vacuo surface analytical studies using both X-ray photoelectron spectroscopy (XPS) and Auger electron spectroscopy (AES), show it to be a mixture of both carbon and silicon carbide. Micro-Raman spectroscopy suggests that the film is amorphous carbon, as opposed to micro-crystalline graphite, however more work is necessary in this area due to the thinness of the layer. Furthermore, at these thicknesses (20 - 50 nm), the relative cross section for silicon carbide is too small for detection by Raman spectroscopy. No faceted structures could be observed by SEM; although future research will involve the study of diamond growth on this amorphous carbon layer with scanning tunneling microscopy and transmission electron microscopy in hopes of better understanding the diamond nucleation process.

Both SEM and Raman spectroscopy were used to determine the quality of the diamond grown on this pretreatment layer (Figures 7a, 7b and 7c). The diamond films shown here were grown on unscratched silicon wafers at 25 Torr in a 1% methane in hydrogen mixture. The total flow rate was 1000 sccm, the substrate temperature was 800 °C and the microwave power was about 750 watts. The pretreatment consisted of biasing the substrate at -250 V relative to ground for 1.5 hours, in a 1% methane mixture at 1000 sccm total flow and 15 Torr. The ion current was measured to be

between 75 and 125 mA during this process. The pretreatment was performed at lower pressures in order to obtain higher ion currents. There appears to be a relationship between the ion current and the time required to grow an appropriate nucleation layer. Future experiments will involve differentiating between the importance of ion flux to the substrate and the energy at which they arrive.

Laser reflection interferometry has proven to be a useful technique in the study of diamond growth processes. The ability to monitor the nucleation and growth rates in real-time makes it possible to perform systematic kinetic studies more accurately, in a fraction of the time. The problem of surface roughness of polycrystalline films has been overcome by growing diamond on a thin amorphous carbon or diamond-like film created by biasing the substrate negatively while it is in the plasma. By preparing the surface in this manner, it is also conceivable that diamond may be grown on irregularly shaped objects, where uniform substrate preparation by conventional methods may be difficult.

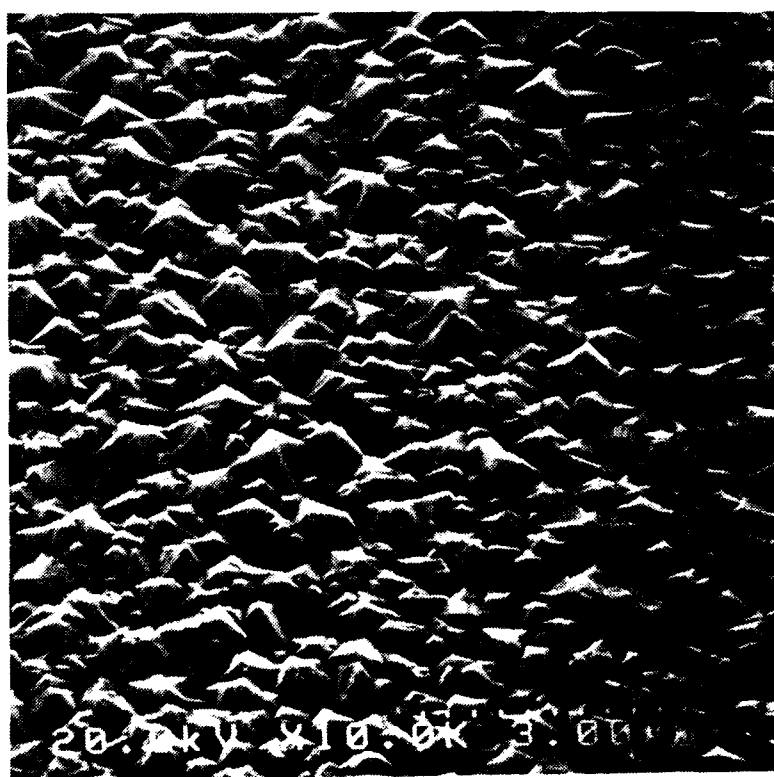


Figure 7a. Surface SEM.



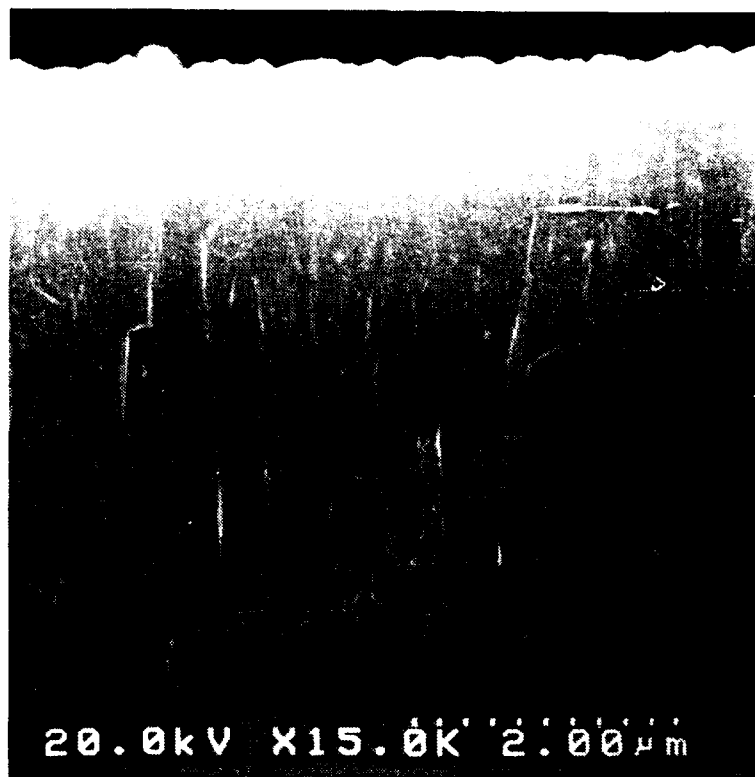


Figure 7b. Cross sectional SEM.

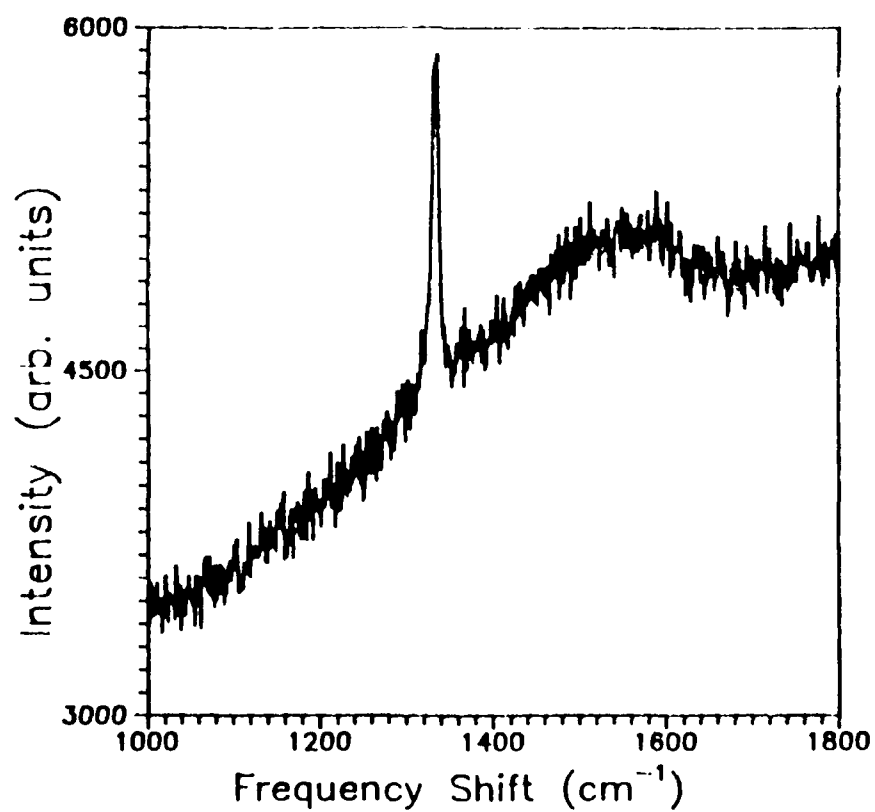


Figure 7(c). Raman spectra of the diamond film grown on the pretreated surface.

The authors wish to acknowledge the partial financial support of SDIO/IST through ONR and Kobe Steel, Ltd. through their Professorship at NCSU. The authors also wish to thank Dr. William Hooke of the University of North Carolina, and Xiao-Hong Wang, of NCSU, for their technical support.

#### References

1. Advance Materials & Processes , 13, (8/89).
2. P. K. Bachman and D.U. Wiechert; Proc. Nato Advanced Study Institute, Castelveccchio, Italy, July 23- Aug. 3, (1990).
3. A. H. Deutchman and R. J. Partyka, Advanced Materials & Processing , 29, (6/89).
4. D. S. Hoover, S-Y Lynn and D. Garg, Solid State Technology, 89, Feb. (1991).
5. A.J. SpringThorpe and A. Majeed, J. Vac. Sci. Technol. B 8 (2)., 266, Mar/Apr, (1990).
6. C. Licoppe, Y. I. Nissim, and C. Meriadec, J. Appl. Phys. 58 (8), 15 . 3094, October (1985).
7. G. L. Olson, S.A. Koborowski, J.A. Roth, R.S. Turley, L.D. Hess, SPIE vol. 276, Optical Characterization Techniques for Semiconductor Technology, 128, 1981)
8. N. Savvides, J. Appl. Phys. 58 (1), 1 July (1985).
9. K. V. Ravi, C. A. Koch, H. S. Hu and A. Joshi, J. Mater. Res., Vol. 5, No. 11, 2356, Nov. (1990).
10. T. Hartnett, R. Miller, D. Montanari, C. Willingham, and R. Tustison, J. Vac. Sci. Tech. A 8 (3), May/Jun (1990), 2129.
11. J.J. Dubray, M. Meloncelli, E. Bertran, C.G. Pantano, "Diamond Nucleation on Silicon, SiAlON and Graphite Substrates Coated with an a-C:H layer", To be published.
12. Richard Post, Astex Co., Personal Communication.
13. S. Yugo, T. Kimura and H. Kanai, 1st. Int. Conf. on the New Diamond Sci. Tech., Tokyo, (1988).
14. S. Yugo, T. Kimura and T. Muto, Vacuum, vol. 41, no. 4-6, 1364, (1990).

### III. Modeling and Characterization of Electronic Devices Fabricated from Semiconducting Diamond Thin Films

#### A. Introduction

Wide bandgap semiconductors such as diamond have the potential to be useful for the fabrication of electronic devices that can operate at high temperature and high power levels in corrosive environments. The high saturation velocity of both electrons and holes in semiconducting diamond thin films indicate that this material should be useful for microwave and millimeter-wave devices. The electron and hole mobilities of this material are sufficiently high that it should be possible to design devices with minimum parasitic resistances. Much of the device potential for diamond is predicted by figure-of-merit calculations that indicate the potential for superior performance in comparison with traditional semiconductor materials such as Si and GaAs. The figure-of-merit calculations are generally formulated using some sort of product between the free carrier saturation velocity, critical electric field for avalanche breakdown, and dielectric constant. As such, the figures-of-merit only give a preliminary and approximate indication of the performance potential of devices fabricated from diamond. More detailed information is available from physical device simulators that can predict the dc and RF potential of the devices from material, device design, and operating condition information.

In this report, a physical device simulator for the microwave MESFET is used to examine the microwave and millimeter-wave potential of MESFET devices fabricated from semiconducting p-type diamond. Due to the relatively high activation energy of boron dopants in diamond ( $E_a \sim 0.37$  eV) it may be necessary to operate the device at elevated temperature. For this reason the operation of the device is considered at both room temperature and 500 °C. The RF performance and design tradeoffs are reported. It is found that p-type diamond MESFETs are capable of significant RF output power, even at elevated temperature.

#### B. Investigation Procedure

A large-signal, numerical model for the MESFET is used for this investigation. The simulator is based upon solutions to the semiconductor device equations and is, therefore, based upon physical device operation. The simulator has previously been used to predict the microwave performance of GaAs microwave MESFETs and has produced results in excellent agreement with experimental data. For this work the simulator was modified to allow for the investigation of diamond devices.

For the study the charge carriers are assumed to be in equilibrium with the lattice at all times so that the Boltzmann equation reduces to the continuity equations for electrons and holes. All transport processes in the semiconductor can then be represented by drift velocities and diffusion coefficients that are functions of the electric field. Poisson's equation is used to relate the carrier concentrations and doping levels in the structure to the electric field. The continuity equations and Poisson's equation are solved by analytical and table look-up techniques.

The model accepts data about the geometry and doping profile of the diode and with the appropriate material data, produces information about the operating characteristics of the device. Both ac and dc solutions are obtained from the model. The MESFET is embedded in a realistic dc and RF circuit so that impedance tuning considerations are included. The principal output data of the RF simulation are the input and output RF impedances, the RF output power, the power-added efficiency, and the gain. By selecting the operating frequency by means of the period of the applied RF voltage the frequency performance of the device can be investigated. In this work the operation frequency was set to 10 GHz.

### C. P-Type Semiconducting Diamond

One problem that is of concern in research directed towards the development of semiconducting diamond electronic devices is the availability of suitable dopants. Theoretical simulations of possible device structures for implementation in diamond indicate that the best microwave and millimeter-wave performance would be expected from devices fabricated from n-type diamond thin films. Suitable dopants for producing these layers have not yet, however, been identified. Suitable device quality synthetic n-type diamond has not yet been demonstrated. Device quality p-type material, however, can be produced using boron as the impurity. This material also looks attractive for fabrication of electronic devices since holes in diamond have good mobility and saturated velocity, only slightly less than that for electrons. A question concerning the use of p-type material relates to the temperature at which the device must operate. Boron in diamond creates an acceptor level with an activation energy that has been reported to vary from  $E_a = 0.013 \text{ eV}$  when introduced by CVD [15],  $E_a = 0.2-0.35 \text{ eV}$  when introduced during growth by high pressure synthesis [16], and  $E_a = 0.27-0.37 \text{ eV}$  when introduced by ion-implantation [17]. The lower activation energies, however, are believed to involve defects, etc. and the generally accepted activation energy for boron in diamond is  $E_a = 0.37 \text{ eV}$ . There is concern that in order to obtain sufficient charge carriers for device applications high operating temperature may be required.

Operation at elevated temperature, however, creates a problem for p-type material in that the hole mobility demonstrates a temperature dependence of approximately  $T^{-2.8}$ . This is in contrast to that for electrons, which follow approximately a  $T^{-1.1}$  law. Operation at elevated temperature for p-type diamond devices is expected, therefore, to result in significantly degraded RF performance.

#### D. Results

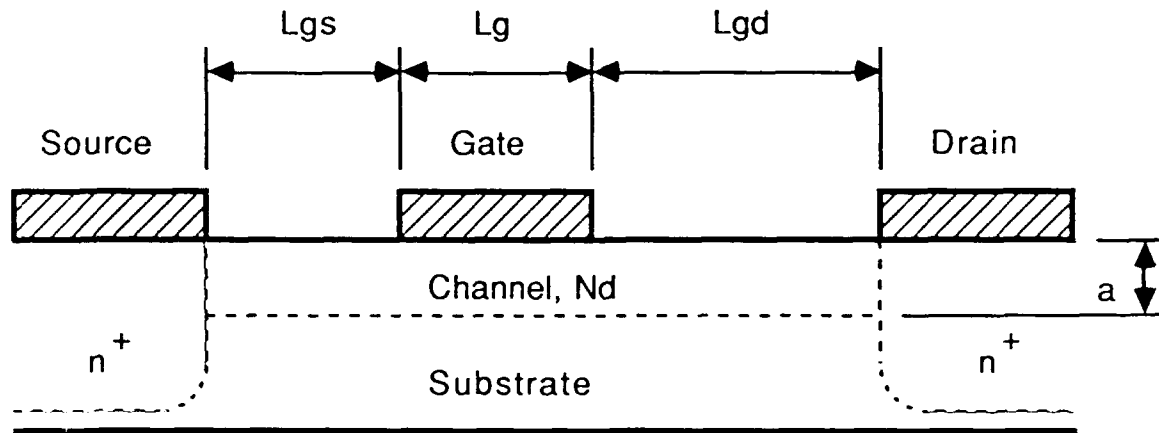
An X-band power MESFET was designed to produce maximum power-added efficiency under class A operating conditions at 10 GHz. The device structure and dimensions and the device and material parameters used in the simulation are shown in Figure 8. The device has a gate length of  $L_g = 0.5 \mu\text{m}$  and a gate width of  $W = 1 \text{ mm}$ . These dimensions are typical of those used for GaAs power MESFETs. The material parameters used for both the room temperature and 500 °C simulations are listed. Full activation was not assumed and the boron doping level would need to be sufficient to result in a channel hole density of  $4 \times 10^{17} \text{ cm}^{-3}$ . The actual boron density could, therefore, be one to three orders of magnitude greater than the hole density. This difference would diminish as the temperature and activation increased. This issue will be investigated in more detail in future simulations.

The dc I-V characteristics for the device at room temperature are shown in Figure 9. For room temperature operation the hole mobility and saturated velocity were  $600 \text{ cm}^2/\text{V-sec}$  and  $1.08 \text{ cm/sec}$ , respectively. As shown in Figure 9 the device has a pinch-off voltage of about -12 v and a maximum transconductance of  $g_m = 52 \text{ mS/mm}$ .

The RF operation of the device was simulated by embedding the device in an RF circuit and tuning the input and output impedances for maximum power-added efficiency at the one db compressed RF output power point. This is generally accomplished by an iterative procedure in which the input is tuned for maximum RF output power when the output is terminated in a conjugate impedance match. This process can be time consuming, but is consistent with the experimental technique commonly used. The simulation procedure is facilitated with the use of a theoretical load-pull algorithm that has been incorporated into the simulator.

The results of the calculations for the 10 GHz, room temperature operation are shown in Figures 10-12. The RF output power versus input power is shown in Figure 10 for three values of drain bias. As expected, the RF output power increases with drain bias. The maximum RF output power at the one db compression point is 37.7 dbm or 5.9 W/mm. This is significantly greater than can be achieved with GaAs MESFETs, which so far have demonstrated about 1.7 W/mm. The gain is shown in Figure 11. With  $V_{ds} = 40 \text{ v}$  about 12 db of gain is obtained. In addition, the linear (or

## *P-Type Diamond MESFET*



Parameter	Value	
	Room Temp.	500 °C
$L_g$	0.5 $\mu\text{m}$	0.5 $\mu\text{m}$
$W$	1 mm	1 mm
$L_{ds}$	1 $\mu\text{m}$	1 $\mu\text{m}$
$L_{gs}$	1 $\mu\text{m}$	1 $\mu\text{m}$
$N_d$	$4 \times 10^{17} \text{ cm}^{-3}$	$4 \times 10^{17} \text{ cm}^{-3}$
$n^+$	$10^{19} \text{ cm}^{-3}$	$10^{19} \text{ cm}^{-3}$
$a$	0.15 $\mu\text{m}$	0.15 $\mu\text{m}$
$\Phi_{bi}(\text{Au})$	1.71 eV	1.68 eV
$R_c$	$\sim 10^{-4} \Omega\text{-cm}^2$	$\sim 10^{-4} \Omega\text{-cm}^2$
$\mu_p$	600 $\text{cm}^2/\text{V-sec}$	100 $\text{cm}^2/\text{V-sec}$
$v_s$	$1.08 \times 10^7 \text{ cm/sec}$	$0.86 \times 10^7 \text{ cm/sec}$
$\Theta$	0.73 °K/W	1.57 °K/W

Figure 8. Device Cross Section and Parameter Values for a P-Type Diamond MESFET.

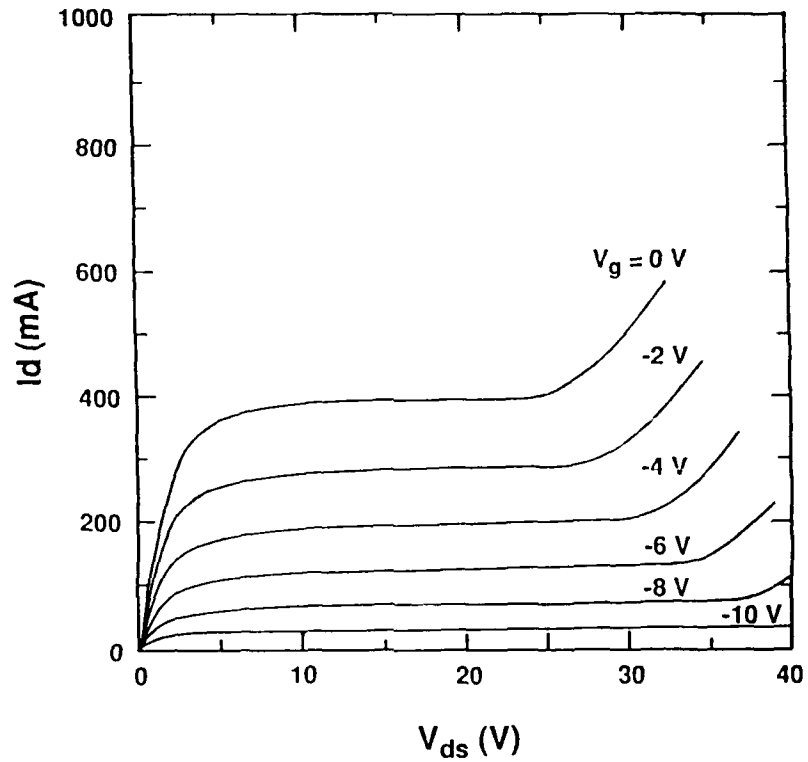


Figure 9. I-V Characteristics for a P-Type Diamond MESFET at Room Temperature.

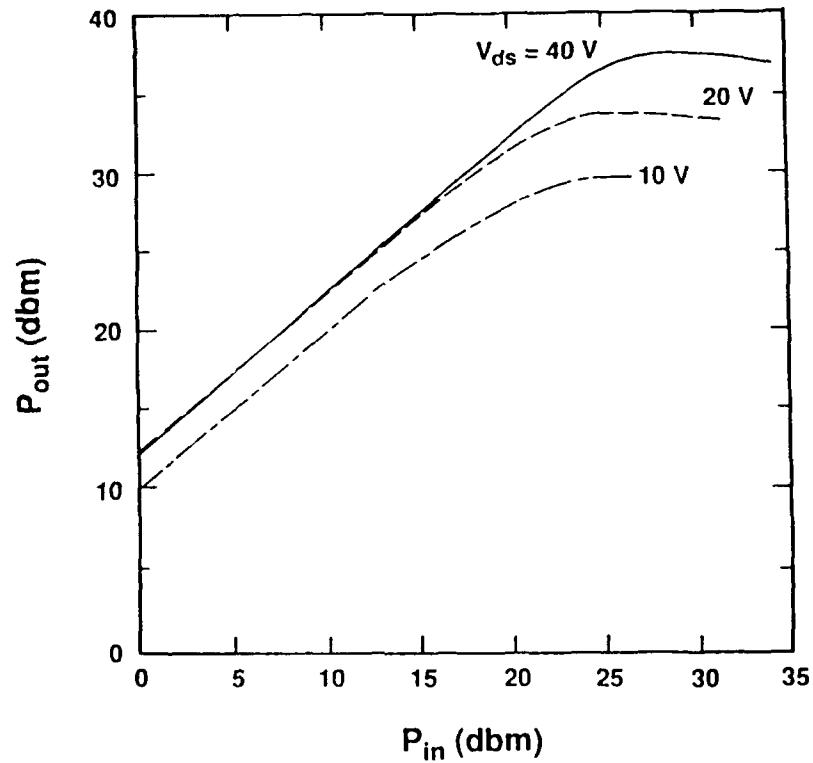


Figure 10. RF Output Power versus Input Power for the P-Type Diamond MESFET at Room Temperature ( $F = 10$  GHz, Class A,  $V_{ds} = 40$  v).

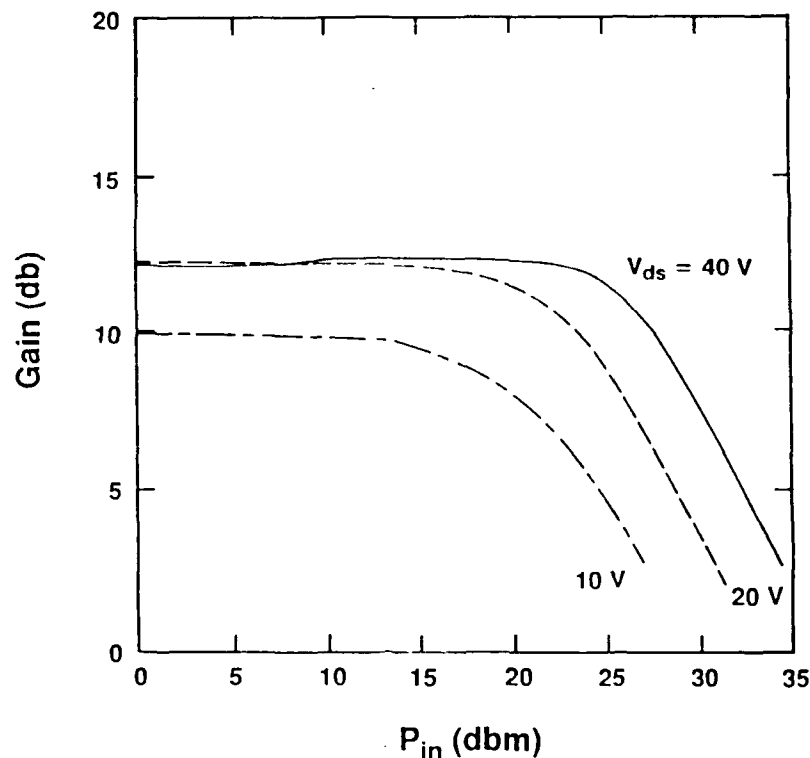


Figure 11. Gain versus Input Power for the P-Type Diamond MESFET at Room Temperature ( $F = 10$  GHz, Class A,  $V_{ds} = 40$  v).

dynamic) range is about 25 db. The power-added efficiency is shown in Figure 12. As indicated, excellent PAE can be obtained and the  $V_{ds} = 40$  v drain bias allows a PAE  $\sim 50\%$  to be achieved. This is at the limit of efficiency expected for class A operation. The excellent performance is obtained due to waveform shaping when the device is driven into saturation. The results are very dependent upon circuit tuning conditions. This process is currently under investigation, but is consistent with both experimental and theoretical calculations obtained with GaAs power devices. The results of the simulations for operation at  $500^\circ\text{C}$  are shown in Figures 13–16. For operation at elevated temperature the hole mobility and saturated velocity are  $100\text{ cm}^2/\text{V-sec}$  and  $0.86 \times 10^7\text{ cm/sec}$ , respectively. The maximum channel current and transconductance that can be achieved are reduced to slightly over 200 mA and about 30 mS/mm, respectively. These reductions scale, of course, directly with the velocity-field characteristics. The RF output power versus input power is shown for drain bias voltages of  $V_{ds} = 30$ , 20, and 10 v in Figure 14. The one db compressed RF output power for the  $V_{ds} = 30$  v bias is  $P_o = 32.8\text{ dbm}$  or 1.9 W/mm. The gain and PAE versus input power for the device are shown in Figures 15 and 16, respectively. The



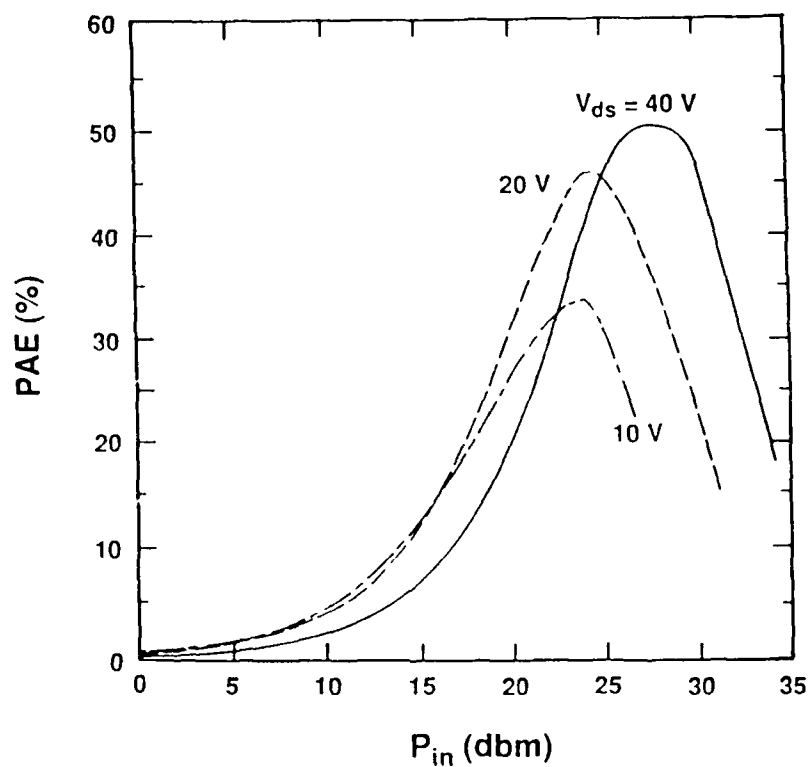


Figure 12. Power-Added Efficiency versus Input Power for the P-Type Diamond MESFET at Room Temperature ( $F = 10$  GHz, Class A,  $V_{ds} = 40$  v).

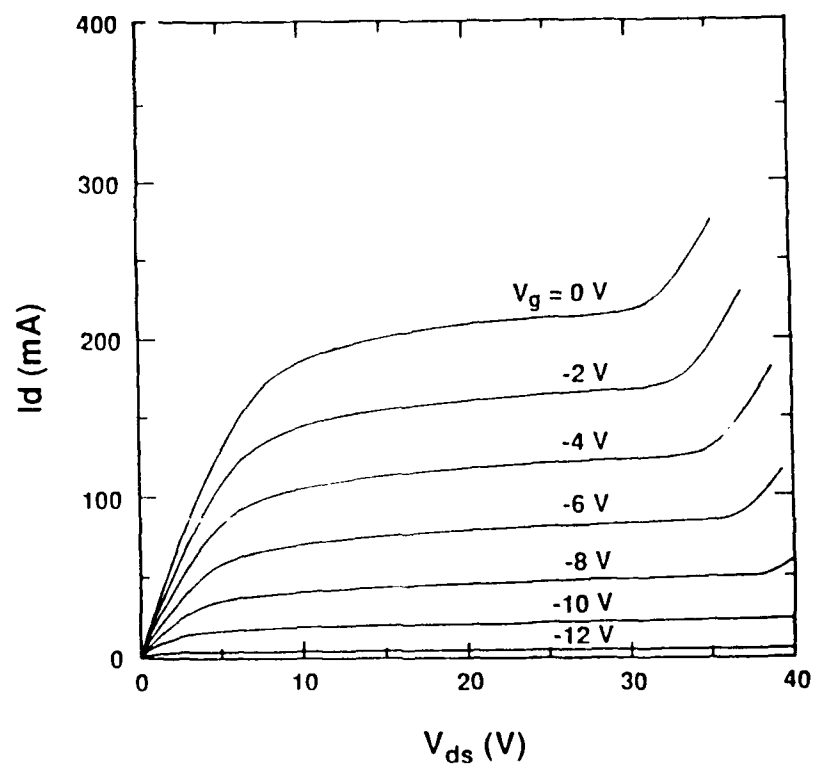


Figure 13. I-V Characteristics for the P-Type Diamond MESFET at 500 °C.

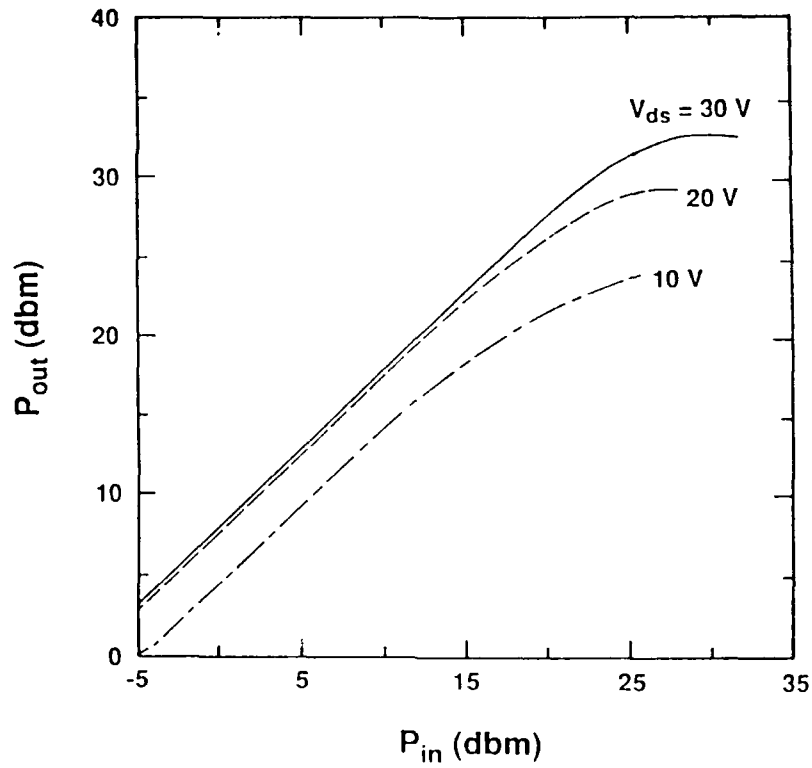


Figure 14. RF Output Power versus Input Power for the P-Type Diamond MESFET at 500 °C ( $F = 10$  GHz, Class A,  $V_{ds} = 30$  v).

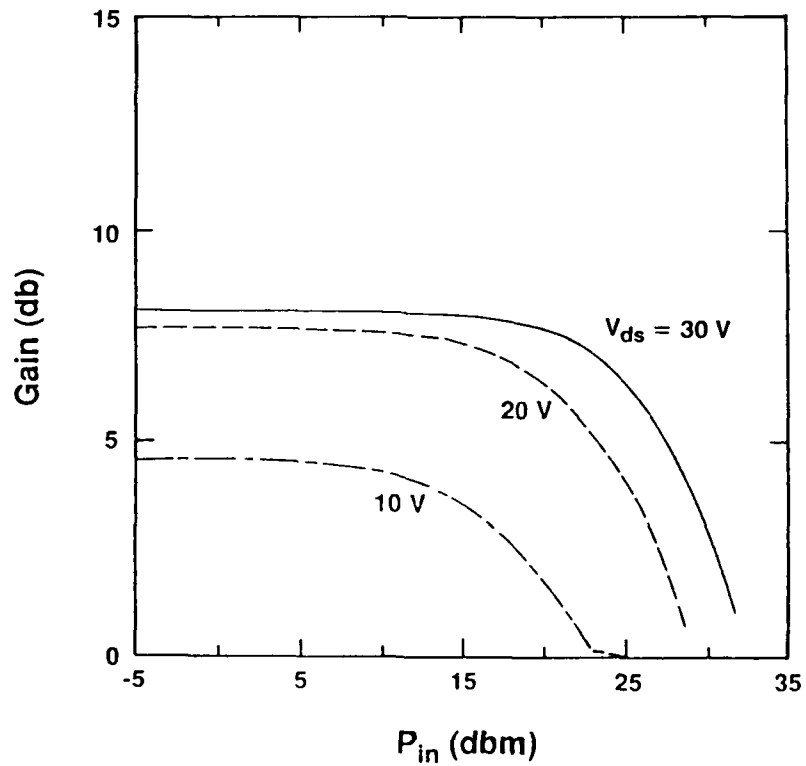


Figure 15. Gain versus Input Power for the P-Type Diamond MESFET at 500 °C ( $F = 10$  GHz, Class A,  $V_{ds} = 30$  v).

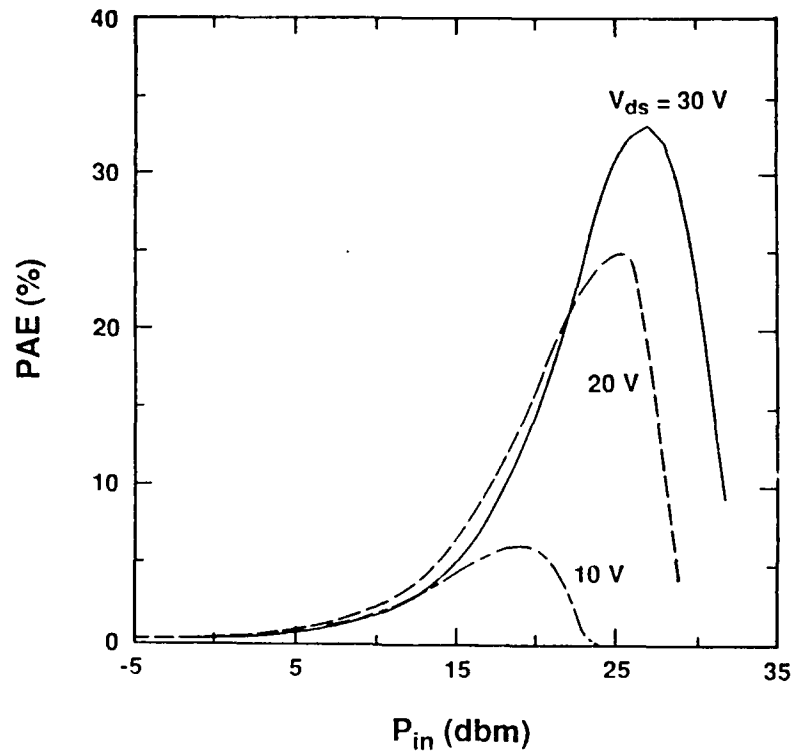


Figure 16. Power-Added Efficiency versus Input Power for the P-Type Diamond MESFET at 500 °C ( $F = 10$  GHz, Class A,  $V_{ds} = 30$  v).

linear gain for the device with the  $V_{ds} = 30$  v bias is about 8 db and the maximum PAE at one db compression is about 33%.

The 500 °C RF performance is significantly reduced from the room temperature results, but is still greater than obtained from GaAs power MESFETs at room temperature. In addition, the GaAs MESFET would not function at 500 °C, but would burn out. This indicates that p-type diamond MESFETs could be used with good RF performance in high temperature applications where currently available devices cannot operate. The room temperature and 500 °C performance are summarized in the following table.

Table I. P-Type Diamond MESFET  
Class A Operation at 10 GHz

Room Temperature	500 °C
$V_{ds} = 40$ v	$V_{ds} = 30$ v
$BV_{gd} = 92$ v	$BV_{gd} = 70$ v
$P_o = 37.7$ dbm	$P_o = 32.8$ dbm
$PAE_{max} = 50.6$ %	$PAE_{max} = 33.2$ %
$G = 12.2$ db	$G = 8.1$ db

### E. Conclusions

The microwave performance of p-type diamond MESFETs operating under class A operation conditions at 10 GHz is investigated. The use of boron dopants allows p-type semiconducting thin films suitable for the fabrication of MESFETs. Boron, however, has a relatively high activation energy and elevated temperature operation may be necessary in order to obtain suitable free charge densities in the MESFET conducting channel. Elevated temperature operation is expected to result in significantly degraded RF performance since holes in diamond demonstrate a  $T^{-2.8}$  temperature dependence. In this study RF operation at room temperature and 500 °C was simulated. The study reveals that although elevated temperature operation results in degradation, the RF performance possible is still significantly superior to that available from GaAs MESFETs operating at room temperature. At 10 GHz and 500 °C the p-type diamond MESFET is capable of producing RF output power, power-added efficiency and gain of 1.9 W/mm, 33 % and 8 db, respectively.

### F. Future Research Plans and Goals

The RF operation of the p-type diamond MESFETs will be investigated in more detail. In particular, the operation of the devices at higher frequencies, up to 100 GHz will be simulated. The dopant activation issue will be investigated in more detail by means of simulations of the density of free charge carriers as a function of temperature. This issue must be addressed, along with the question of gate-drain breakdown voltage in order to obtain a realistic picture of the potential of these devices for microwave and mm-wave applications.

### G. References

15. N. Fujimori, T. Imai and A. Doi, *Vacuum*, vol. 36, no. 1-3, p. 99, 1986
16. R.H. Wentorf, *J. Chemical Phys.*, vol. 36, p. 1987, April 1962.
17. V.S. Vavilov, M.A. Gukasyan, M.I. Guseva, T.A. Karatyginal and E.A. Konorova, *Sov. Phys. Semicond.*, vol. 8, p. 471, Oct. 1974.